HHS Public Access

Author manuscript

Burns. Author manuscript; available in PMC 2016 August 01.

Published in final edited form as:

Burns. 2015 August ; 41(5): 1058–1063. doi:10.1016/j.burns.2014.11.018.

Acute discrimination between superficial-partial and deep-partial thickness burn injuries in a preclinical model with laser speckle imaging

Christian Crouzet[a,b], **John Quan Nguyen**[a], **Adrien Ponticorvo**[a], **Nicole P. Bernal**[c], **Anthony J. Durkin**[a,c], and **Bernard Choi**[a,b,c,d]

[a]Beckman Laser Institute and Medical Clinic, University of California, Irvine, CA 92612

[b]Department of Biomedical Engineering, University of California, Irvine, CA 92697

[c]Department of Surgery, University of California, Irvine, CA 92868

[d]Edwards Lifesciences Center for Advanced Cardiovascular Technology, University of California, Irvine, CA 92697

Abstract

A critical need exists for a robust method that enables early discrimination between superficial-partial and deep-partial thickness burn wounds. In this study, we report on the use of laser speckle imaging (LSI), a simple, non-invasive, optical imaging modality, to measure acute blood flow dynamics in a preclinical burn model. We used a heated brass comb to induce burns of varying severity to nine rats and collected raw speckle reflectance images over the course of three hours post burn. We induced a total of 12 superficial-partial and 18 deep-partial thickness burn wounds. At three hours post burn we observed a 28% and 44% decrease in measured blood flow for superficial-partial and deep-partial thickness burns, respectively, and that these reductions were significantly different ($p = 0.00007$). This preliminary data suggests the potential role of LSI in the clinical management of burn wounds.

Keywords

laser speckle imaging; preclinical model; superficial-partial thickness; deep-partial thickness; burn wounds

Corresponding author. Bernard Choi, Ph.D., University of California, Irvine, Beckman Laser Institute and Medical Clinic, 1002 Health Sciences Road East, Irvine, CA 92612, choib@uci.edu, Phone: +1 949 824-9491, Fax: +1 949 824-6969.

1. Introduction

1.1 Clinical Evaluation

According to the American Burn Association, 450,000 people receive medical attention for burn wounds, with 40,000 requiring hospitalization and 3,400 deaths attributed to burn wounds [1]. Typical causes of burn wounds include flame, hot water, electricity, and chemicals [2]. Clinical observation is the most common method of diagnosing the severity of a burn wound [3]. The clinician performs tests that provide visual and tactile information of the burn wound, such as wound appearance (edema, color, and blisters), capillary blanching and refill, and sensibility to pinprick and touch [4].

Based on this information, the clinician typically categorizes the burn wound into one of four categories: superficial, superficial-partial, deep-partial, or full thickness burns. Each category is associated with varying healing periods and characteristics. Superficial burn wounds only involve injury of the epidermis and are associated with hyperemia, a dry surface, a diffuse pink or red color, and an absence of blisters. These wounds heal within fourteen days. Full thickness burn wounds involve injury of the epidermis, dermis, and hypodermis; and are associated with thrombosis; a dry, leathery, and rigid appearance; a white, black, and cherry red color; and an absence of blanching with pin pricks. These wounds take longer than 21 days to heal [5].

While superficial and full thickness burns are straightforward to diagnose based on visual appearance, clinicians have difficulty with accurate differentiation between superficial-partial and deep-partial thickness burns. The experience of the clinician and the fact that these burns can dynamically increase in severity (i.e., burn wound conversion) during the initial 48 hour period, both lead to higher clinician error [4]. Both wound types are associated with similar characteristics, and both involve the epidermis and dermis. Superficial-partial burns involve injury of the papillary dermis and are associated with intact blisters, moderate edema, a moist surface under the blisters, a bright pink or red color, and blanching with fast capillary refill after pressure is applied. Deep-partial thickness burns involve injury of both the papillary and reticular dermis and are associated with broken blisters, substantial edema, a wet surface, a mixed red or waxy white color, and blanching with slow capillary refill after pressure is applied [5].

With superficial or superficial-partial burn wounds, patients receive antimicrobial creams for treatment. With deep-partial or full thickness burn wounds, excision and grafting are required [6]. The decision on treatment protocol is typically based on clinical observation and hence remains subjective. Unfortunately, the reported accuracy of this approach is ~67% [4]. Hence, a critical need exists to develop technologies and methodologies that improve the accuracy of burn-wound assessment. Recently, we reviewed various technologies that have been investigated within the context of burn wound severity assessment [7]. One set of techniques that appears to be promising in this regard is based on measurements of skin blood flow.

1.2 Laser Doppler Imaging

Researchers have studied the use of laser Doppler imaging (LDI) to assess burn wounds. Stern first demonstrated that LDI provides measurements related to the Doppler shift resulting from interactions of incident coherent light with moving red blood cells [8]. With LDI, researchers have reported accuracies greater than 90% after 72 hours post-burn [9,10,11], demonstrating the potential efficacy of LDI to characterize burn wounds.

Despite the high accuracy associated with LDI, it unfortunately remains largely a research tool, in part because of limitations including long scan times, cost, system size, and artifacts associated with patient movement [7]. Laser speckle imaging (LSI) is a relatively low-cost approach to gather similar blood-flow information that offers faster acquisition speeds, day-to-day reproducibility [12], and simple instrumentation [13]. We previously used LSI for several biomedical applications [14–17]. In the present work, we characterized the performance of LSI to evaluate perfusion dynamics associated with burn wounds of graded severity. Based on the results from several studies using LDI [9,11,18,19], our central hypothesis was that a decrease in blood-flow values measured with LSI correlate with increasing burn severity, and hence enable differentiation of superficial-partial and deep-partial thickness burns.

2. Materials and Methods

2.1 Animal Model

We performed experiments involving nine male Sprague Dawley rats (300 to 400g in mass). The burn model and study protocol (#1999–2064) were approved in accordance with the University of California, Irvine Institutional Animal Care and Use Committee.

2.2 Burn Wounds

We used an identical burn wound protocol to one we described previously [20]. Briefly, burn wounds were induced using a previously established brass comb [21] that consisted of four prongs each 10 × 20 mm with 5 mm gaps between each prong, as shown in figure 1.

One day prior to burn induction, rats were shaved on the lateral dorsal region and Nair (Church and Dwight, Princeton, NJ) was applied to remove excess hair. The rats were anesthetized with a combination of ketamine hydrochloride (0.87 mL/kg) and xylazine (0.65 mL/kg) via intraperitoneal (i.p.) injection, with booster injections used as necessary. The brass comb was immersed in 100°C boiling water and applied to the hairless lateral dorsal region without any additional applied force other than gravity. Burn times ranged from two to ten seconds with the intent of creating burn severities of superficial-partial and deep-partial thickness burns.

During the three hours after burn wounds were created, images were acquired approximately every 20 to 25 minutes. The rats were then euthanized with Euthasol via i.p. injection. A skin pelt of the burned region from the lateral dorsal side of each rat was removed and placed into 10% buffered formalin for 24 hours, followed by dehydrating and embedding the tissue in paraffin. Cuts were then made with a microtome to separate and examine each burn

site individually. A vertical section was then cut through the middle of each burned region that bisected each burn site along the long axis from top to bottom. Normal skin was also taken sufficiently far from the burned region, to not be affected by the burn induction, yet still be taken from the lateral dorsal region of the rat. Normal sections and burn severity were verified using hematoxylin and eosin (H&E) staining and optical microscopy (Olympus BH2, Tokyo, Japan).

2.3 LSI Instrumentation, Data Acquisition and Analysis

For an excitation source, we used an 808nm laser (Ondax, Monrovia, CA) with the collimator removed. We used a ground glass diffuser (ThorLabs, Inc., Newton NJ) to expand the beam and achieve near-uniform illumination of the tissue (figure 2). For each image collection timepoint, we used a multispectral CCD camera (Nuance, Cri, Inc., Woburn, MA) to collect 50 raw speckle images with an exposure time of 10ms.

We used custom-written MATLAB code (MathWorks Inc., Natick, MA) to process the raw speckle images. We used a sliding 5×5 square structuring element to convert each raw image to a corresponding speckle contrast image. The following operation was performed at each location of the structuring element:

$$K=\frac{v}{<l>} \quad \text{Eq. 1}$$

To account for motion artifact associated with breathing that is evident with visual inspection of the image sequences, we selected, in an automated fashion, five speckle contrast images with the highest average contrast value. This approach was based on the assumption that motion reduces artificially speckle contrast, and the images acquired without motion also will have the highest speckle contrast. From these five images, we calculated a single average speckle contrast image, which we then converted to a Speckle Flow Index (SFI) map using a simplified speckle imaging equation [22]:

$$SFI=\frac{1}{2TK^2} \quad \text{Eq. 2}$$

We then selected regions of interest (ROIs) from which we calculated average SFI values. To account for the potential heterogeneity in burn severity within each burn region, we selected ROIs that corresponded to the regions from which histological analysis was performed. We set each ROI to have the same number of pixels. In the pre-burn imaging data, we also selected a ROI corresponding to the eventual location of the four burn sites to serve as a representative measure of baseline SFI values. We applied a box-and-whisker test to remove outliers from the resultant data set, resulting in rejection of one burn site from further consideration.

2.4 Statistical Analysis

We used a t-test to compare the SFI values of burn wounds with superficial-partial and deep-partial thickness burn severities, at each timepoint. A p-value less than 0.05 was considered statistically significant for this study.

3. Results

3.1 Histology

Burn severities were assessed using H&E staining and optical microscopy. One of the co-authors (NPB) assessed, in a blinded fashion, burn depth associated with each histological section, in accordance with thermal-damage features reported in the literature [23]. Burns were examined by observing hair follicle and sweat gland denaturation, along with the glass-like appearance of collagen. Examples of normal skin, superficial-partial and deep-partial thickness burn severities are shown in figure 3. In this study, 12 superficial-partial and 18 deep-partial thickness burns were obtained.

3.2 SFI Maps and Time Plots

Based on visual inspection alone of the color reflectance images, we did not observe any visual changes that enabled clear differentiation among levels of burn severity (figure 4). Based on visual inspection of the SFI maps, we observed on average a larger reduction in SFI values in the deep-partial thickness sites than in the superficial-partial thickness sites.

From a quantitative perspective, the differences between average SFI values taken from the superficial-partial and deep-partial thickness sites, are statistically significant ($p<0.05$) at all measurement time-points collected during the first three hours following burn wound induction (figure 5). At the three hour timepoint, the SFI values in the superficial-partial thickness sites were ~370 lower (28% reduction) than at baseline, and the values in the deep-partial thickness sites were ~580 lower (44% reduction).

Discussion

Our data collectively demonstrates the ability of LSI to discriminate, at early time points (within three hours post burn), between burn wounds of superficial-partial and deep-partial thickness (figures 4 and 5). Compared to LDI, which is the optical technology most frequently used in research studies of burn wounds, LSI has several potential advantages including speed of image acquisition, cost, and portability.

Few published studies [24–27] report on the use of LSI for characterization of burn wounds. Stewart *et al.* [27] measured perfusion of burn scars with LSI and LDI and determined that the two technologies measured similar changes in perfusion ($r^2 = 0.86$). Ganapathy *et al.* [26] combined LSI and optical coherence tomography (OCT) to distinguish among acute (one hour post-burn) burn severities of superficial, partial, and full thickness. With LSI alone and in combination with OCT, they estimated accuracies of 78 and 86%, respectively. Unfortunately, they did not assess the efficacy of LSI to differentiate between superficial-partial and deep-partial thickness burn wounds, which oftentimes is the most difficult diagnosis that burn-care specialists need to make.

Lindahl *et al.* [25] used LSI in a clinical study over the course of 14 days and assessed the correlation between longitudinal LSI measurements of perfusion and with one of two outcomes 1) healed within 14 days; and 2) healed after 14 days, or required surgery. Their data suggest that early (0 to 7 days post burn) LSI measurements of perfusion can

distinguish between burns that healed within 14 days and those that healed after 14 days or required surgery. Although Lindahl *et al.* did not report on differentiation among different severities of burn wounds, their data suggest the ability of LSI to monitor the healing of burn wounds in a clinical setting.

Collectively, the published data that we cite above and the data that we present in this study (figures 3–5), suggest the potential of LSI to characterize the severity of burn wounds as early as the first three hours post burn. Although we detected statistically-significant differences in perfusion dynamics between superficial-partial and deep-partial thickness burns, future work will include a study to determine the degree to which these acute change are indicative of future healing outcomes. Due to the acute nature of the study, this study does not allow for the analysis of burn wound conversion, where more superficial burns can become deeper. This can then lead to unstable skin and hypertrophic scar formation [28]. However, the results presented here suggest that LSI can still provide clinicians with a valuable tool that can be used for early burn wound severity examination. We acknowledge that translation of our results to clinically-relevant outcomes is complicated by the differences between rat skin and human skin. Rat skin is two to 10 times thinner than human skin [29]. Our study specifically involved contact burn injuries, but flame, electric, and chemical injuries also exist as previously mentioned; the perfusion dynamics may differ for different types of burn wounds.

Even with these limitations, we conclude that the *in-vivo* data presented in this study represent an important first step to develop a noninvasive optical tool that can reliably distinguish between superficial-partial and deep-partial thickness burn wounds. Integration of LSI and other optical imaging methods, such as Spatial Frequency Domain Imaging [20], is expected to yield a device that enables robust characterization of the severity of burn wounds. Such a multimodal device is expected to improve the accuracy of LSI-based estimates of tissue perfusion associated with highly dynamic environments such as burn wounds [30,31].

Acknowledgements

We gratefully acknowledge support from the Beckman Foundation and the NIH, including P41EB015890 (A Biomedical Technology Resource) and the Military Medical Photonics Program (AFOSR FA9550-10-1-0538). The content is solely the responsibility of the authors and does not necessarily represent the official views of the NIH.

References

1. Burn Incidence and Treatment in the United States: 2013 Fact Sheet. 2014 Apr 16. [Accessed]: http://www.ameriburn.org/resources_factsheet.php.
2. Hettiaratchy S, Dziewulski P. ABC of burns – Introduction. BMJ. 2004; 238:1366–1368. [PubMed: 15178618]
3. Heimbach D, Engrav L, Grube B, Marvin J. Burn depth: a review. World J Surg. 1992; 16:10–15. [PubMed: 1290249]
4. Monstrey S, Hoeksema H, Verbelen J, Pirayesh A, Blondeel P. Assessment of burn depth and burn wound healing potential. Burns. 2008; 34:761–769. [PubMed: 18511202]
5. Hettiaratchy S, Papini R. ABC of burns – Initial management of a major burn: II – assessment and resuscitation. BMJ. 2004; 329:101–103. [PubMed: 15242917]

6. Papini R. Management of burn injuries of various depths. BMJ. 2004; 329:158–160. [PubMed: 15258073]
7. Kaiser M, Yafi A, Cinat M, Choi B, Durkin AJ. Noninvasive assessment of burn wound severity using optical technology: a review of current and future modalities. Burns. 2011; 37:377–386. [PubMed: 21185123]
8. Stern MD. In vivo evaluation of microcirculation by coherent light scattering. Nature. 1975; 254:56–58. [PubMed: 1113878]
9. Monstrey SM, Hoeksema H, Baker RD, Jeng J, Spence RS, Wilson D, Pape SA. Burn wound healing time assessed by laser Doppler imaging. Part 2: validation of a dedicated colour code for image interpretation. Burns. 2011; 37:249–256. [PubMed: 21084164]
10. Stewart TL, Ball B, Schembri PJ, Hori K, Ding J, Shankowsky HA, Tredget EE. The use of laser Doppler imaging as a predictor of burn depth and hypertrophic scar postburn injury. J Burn Care Res. 2012; 33:764–771. [PubMed: 22955162]
11. Hoeksema H, Van de Sijpe K, Tondu T, Hamdi M, Van Landuyt K, Blondeel P, Monstrey S. Accuracy of early burn depth assessment by laser Doppler imaging on different days post burn. Burns. 2009; 35:36–45. [PubMed: 18952377]
12. Roustit M, Cracowski JL. Non-invasive assessment of skin microvascular function in humans: an insight into methods. Microcirculation. 2012; 19:47–64. [PubMed: 21883640]
13. Boas DA, Dunn AK. Laser speckle contrast imaging in biomedical optics. J Biomed Opt. 2010; 15:011109. [PubMed: 20210435]
14. Sharif SA, Taydas E, Mazhar A, Rahimian R, Kelly KM, Choi B, Durkin AJ. Noninvasive clinical assessment of port-wine stain birthmarks using current and future optical imaging technology: a review. Br J Dermatol. 2012; 167:1215–1223. [PubMed: 22804872]
15. White SM, Hingorani R, Arora RP, Hughes CC, George SC, Choi B. Longitudinal in vivo imaging to assess blood flow and oxygenation in implantable engineered tissues. Tissue Eng Part C Methods. 2012; 18:697–709. [PubMed: 22435776]
16. Moy WJ, Patel SJ, Lertsakdadet BS, Arora RP, Nielsen KM, Kelly KM, Choi B. Preclinical in vivo evaluation of NPe6-mediated photodynamic therapy on normal vasculature. Lasers Surg Med. 2012; 44:158–162. [PubMed: 22334298]
17. White SM, George SC, Choi B. Automated computation of functional vascular density using laser speckle imaging in a rodent window chamber model. Microvasc Res. 2011; 82:92–95. [PubMed: 21419785]
18. McGill DJ, Sorensen K, MacKay IR, Taggart I, Watson SB. Assessment of burn depth: a prospective, blinded comparison of laser Doppler imaging and videomicroscopy. Burns. 2007; 33:833–842. [PubMed: 17614206]
19. Riordan CL, McDonough M, Davidson JM, Corley R, Perlov C, Barton J, Guy J, Nanney LB. Noncontact laser Doppler imaging in burn depth analysis of the extremities. J Burn Care Rehabil. 2003; 24:177–186. [PubMed: 14501410]
20. Nguyen JQ, Crouzet C, Mai T, Riola K, Uchitel D, Liaw LH, Bernal N, Ponticorvo A, Choi B, Durkin AJ. Spatial frequency domain imaging of burn wounds in a preclinical model of graded burn severity. J Biomed Opt. 2013; 18:066010.
21. Singer AJ, McClain SA, Romanov A, Rooney J, Zimmerman T. Curcumin reduces burn progression in rats. Acad Emerg Med. 2007; 14:1125–1129. [PubMed: 18045885]
22. Ramirez-San-Juan JC, Ramos-Garcia R, Guizar-Iturbide I, Martinez-Niconoff G, Choi B. Impact of velocity distribution assumption on simplified laser speckle imaging equation. Opt Express. 2008; 16:3197–3203. [PubMed: 18542407]
23. Meyerhoz DK, Piester TL, Sokolich JC, Zamaba GK, Light TD. Morphological parameters for assessment of burn severity in an acute burn injury rat model. Int J Exp Pathol. 2009; 90:26–33. [PubMed: 19200248]
24. Stewart CJ, Gallant-Behm CL, Forrester K, Tulip J, Hart DA, Bray RC. Kinetics of blood flow during healing of excisional full-thickness skin wounds in pigs as monitored by laser speckle perfusion imaging. Skin Res Technol. 2006; 12:247–253. [PubMed: 17026655]
25. Lindahl F, Tesselaar E, Sjöberg F. Assessing paediatric injuries using Laser Speckle Contrast Imaging. Burns. 2013; 39:662–666. [PubMed: 23092702]

26. Ganapathy P, Tamminedi T, Qin Y, Nanney L, Cardwell N, Pollins A, Sexton K, Yadegar J. Dual-imaging system for burn depth diagnosis. Burns. 2014; 40:67–81. [PubMed: 23790396]

27. Stewart CJ, Frank R, Forrester KR, Tulip J, Lindsay R, Bray RC. A comparison of two laser-based methods for determination of burn scar perfusion: laser Doppler versus laser speckle imaging. Burns. 2005; 31:744–752. [PubMed: 16129229]

28. Singh V, Devgan L, Bhat S, Milner SM. The pathogenesis of burn wound conversion. Ann Plast Surg. 2007; 59:109–115. [PubMed: 17589272]

29. Pappinen S, Hermansson M, Kuntsche J, Somerharju P, Wertz P, Urtti A, Suhonen M. Comparison of rat epidermal keratinocyte organotypic culture (ROC) with intact human skin: lipid composition and thermal phase behavior of the stratum corneum. Biochim Biophys Acta. 2008; 1778:824–834. [PubMed: 18211819]

30. Mazhar A, Cuccia DJ, Rice TB, Carp SA, Durkin AJ, Boas DA, Choi B, Tromberg BJ. Laser speckle imaging in the spatial frequency domain. Biomed Opt Express. 2011; 2:1553–1563. [PubMed: 21698018]

31. Rice TB, Konecky SD, Mazhar A, Cuccia DJ, Durkin AJ, Choi B, Tromberg BJ. Quantitative determination of dynamical properties using coherent spatial frequency domain imaging. J Opt Soc Am A Opt Image Sci Vis. 2011; 28:2108–2114. [PubMed: 21979516]

Highlights

- We characterized laser speckle imaging (LSI) in a preclinical burn wound model.
- LSI obtained blood-flow information of superficial-partial and deep-partial thickness burn wounds.
- Blood-flow of superficial-partial and deep-partial burns differed significantly.
- Results suggest the use of LSI to clinically evaluating burn wounds.

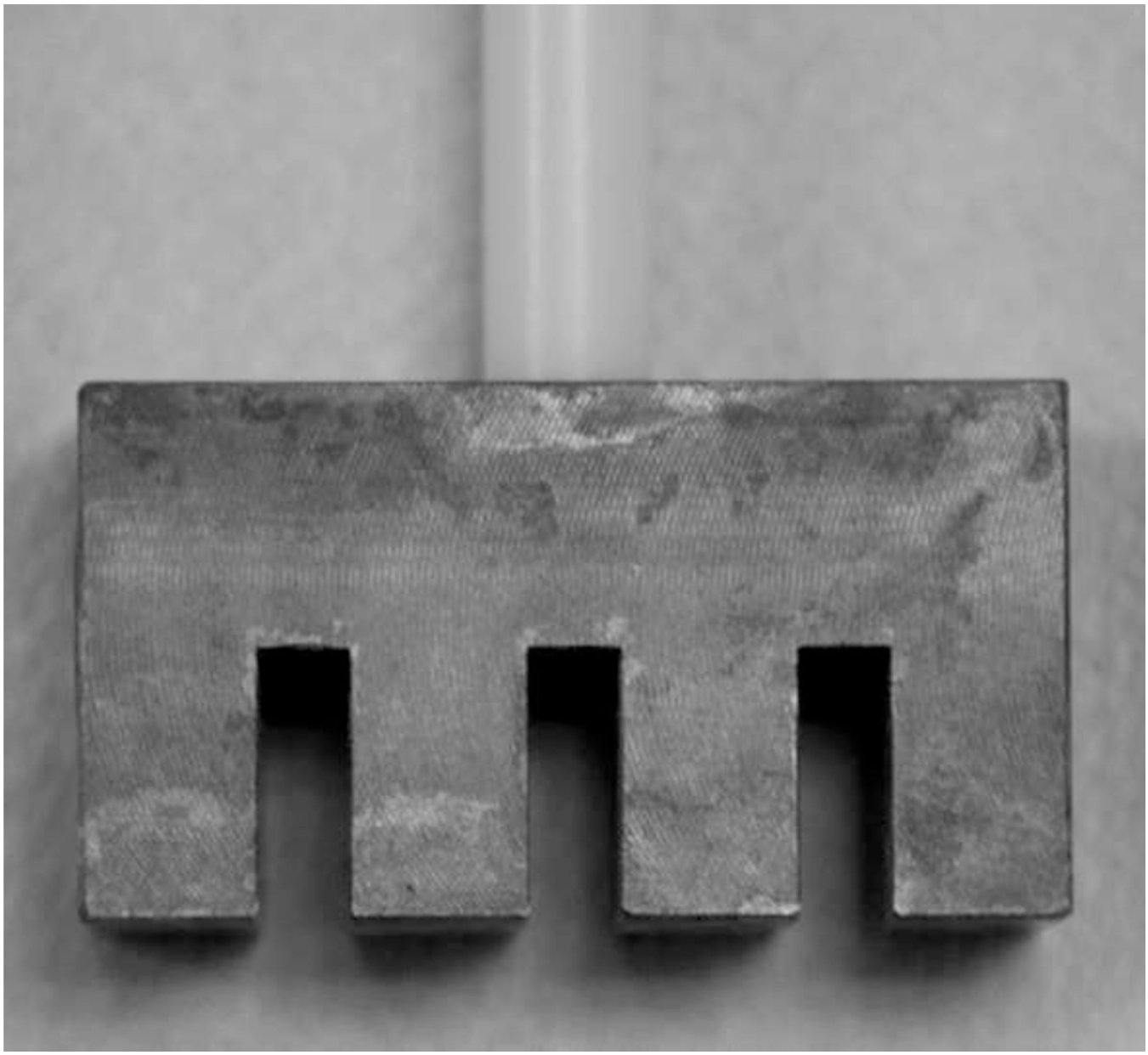

Figure 1.
Brass comb used for burn induction.

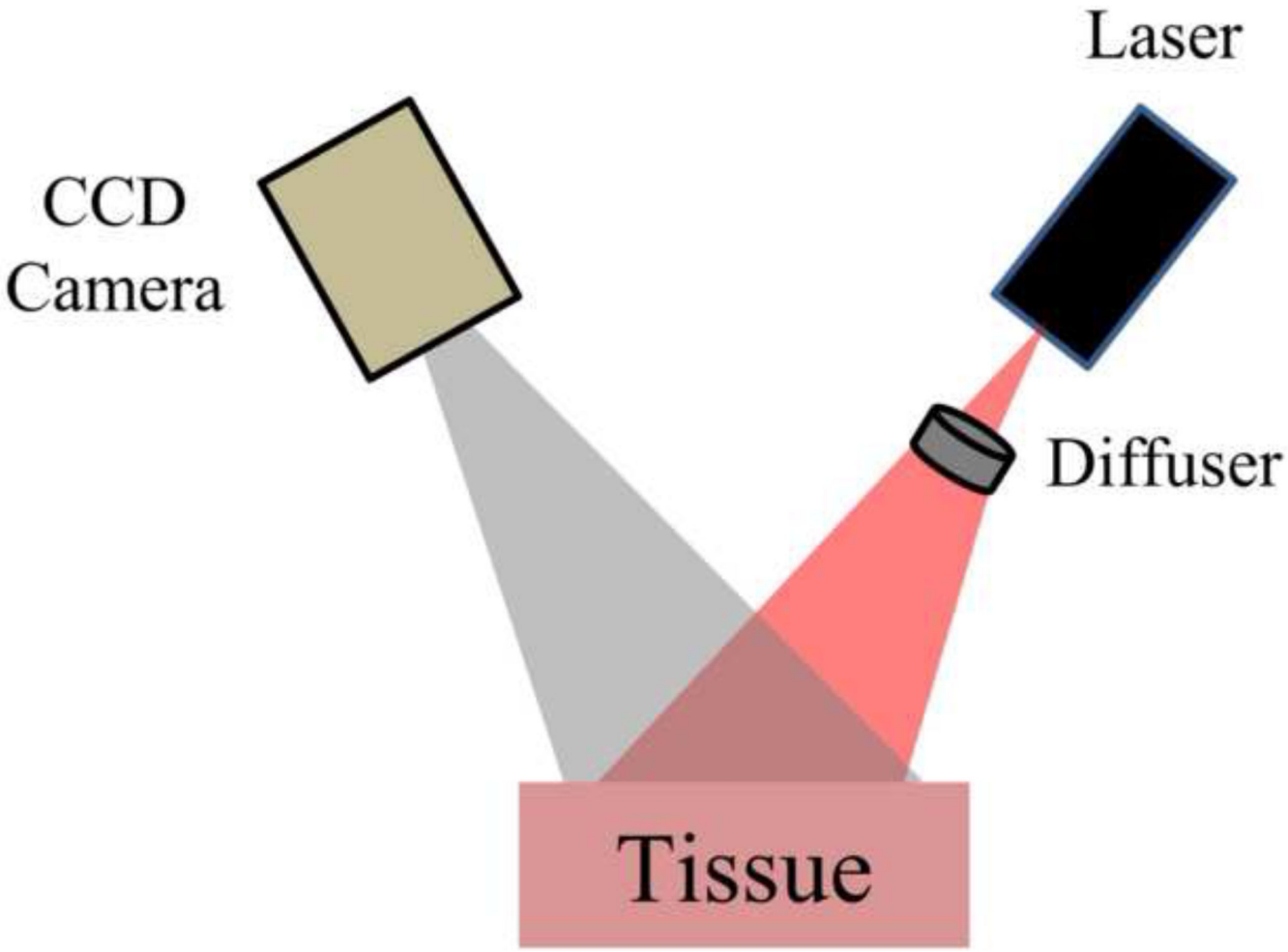

Figure 2.
Schematic of LSI setup.

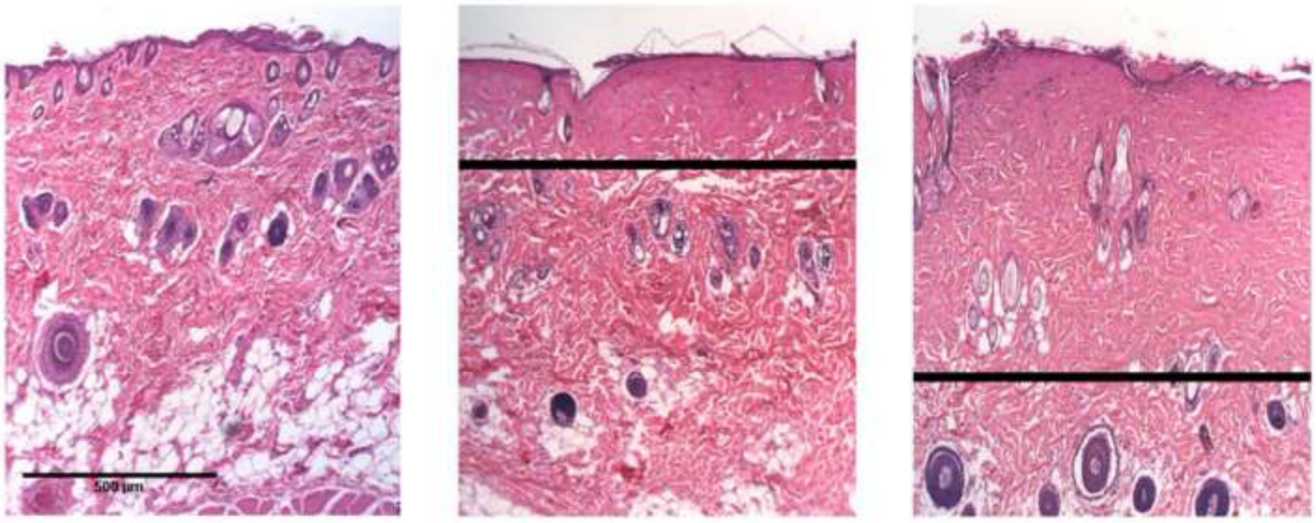

Figure 3.

Representative H&E-stained histological sections for normal skin (left), superficial-partial (middle), and deep-partial (right) thickness burn severities. The black line in the burn wound images represents the estimated burn depth, based on histological markers such as collagen hyalinization and structural alterations to hair follicles. Scale bar = 500μm.

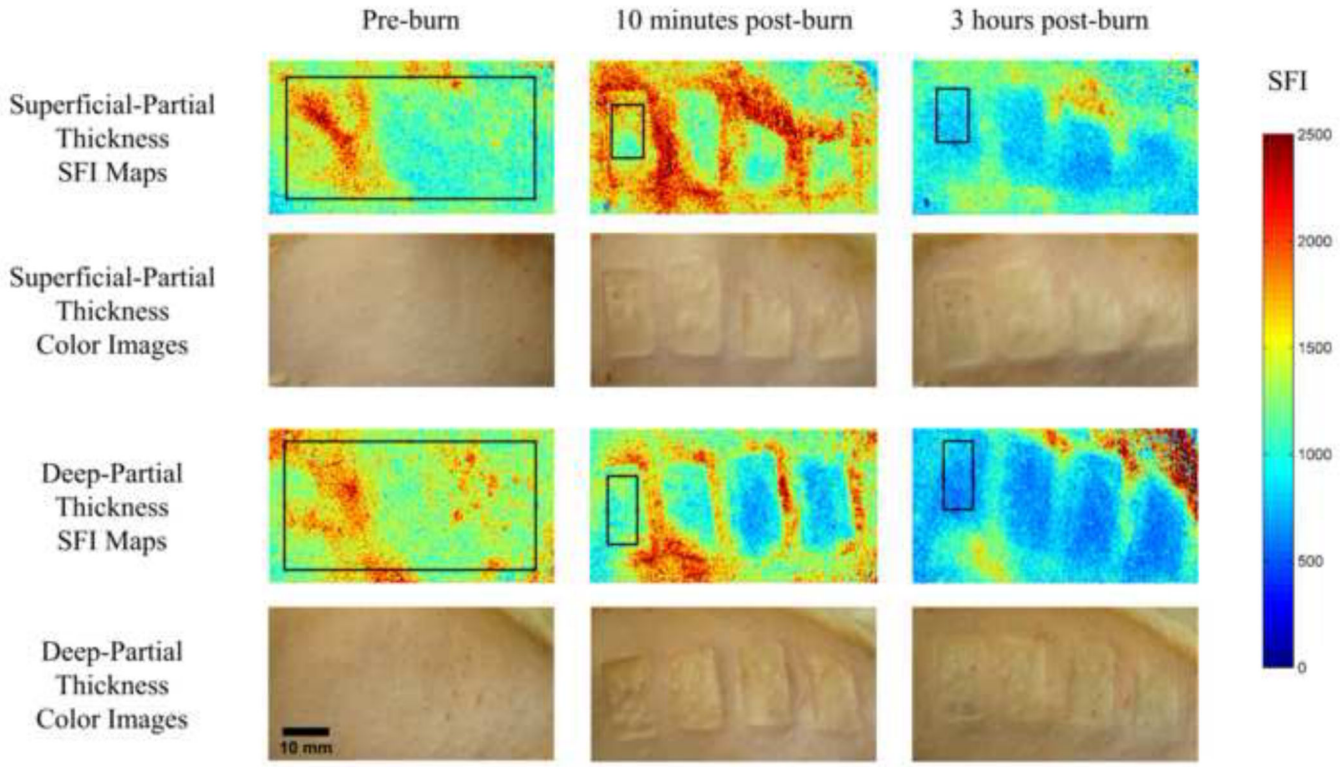

Figure 4.

SFI maps and corresponding color images of superficial-partial (top) and deep-partial (bottom) thickness burns before the burn is induced, 10 minutes, and 3 hours post-burn. The black rectangles represent ROIs that were used for subsequent quantitative analysis. Scale bar = 10 mm.

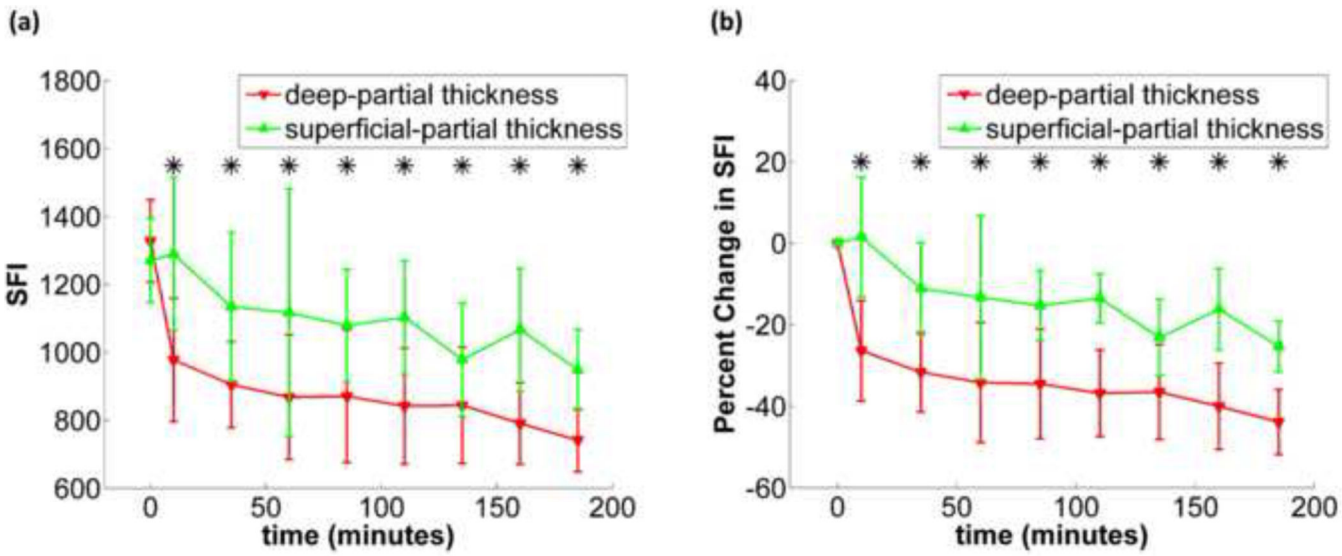

Figure 5.

(a) (left) shows the time plot of average SFI during the experiment for superficial-partial and deep-partial thickness burns with standard deviation error bars, (b) (right) shows the time plot of average percent change in SFI during the experiment for superficial-partial and deep-partial thickness burns with standard deviation error bars. Time points marked with an asterisk are considered statistically significant.